WARSAW UNIVERSITY OF TECHNOLOGY Index 351733
FACULTY OF CIVIL ENGINEERING
COMMITTEE FOR CIVIL AND WATER ENGINEERING
POLISH ACADEMY OF SCIENCES ISSN 1230-2945

DOI: 10.24425/ace.2021.138066

ARCHIVES OF CIVIL ENGINEERING

Vol. LXVII ISSUE 3 2021

s. 469–488

Research paper

Engineering forecasting of the local scour around the circular bridge pier on the basis of experiments

S. Bajkowski[1], M. Kiraga[2], J. Urbański[3]

Abstract: The aim of the study was to indicate the procedure of using laboratory physical model tests of scour around bridge piers for the purposes of determining the potential scour of a riverbed on field bridge crossings. The determination of the uniform modeling scale coefficient according to the criterion of reliable sediment diameter limits the application of the results of tests on physical models to selected types of sediment. The projected depths of scouring of the riverbed at the pier in nature were determined for an object reproduced in the scale of 1:15 determined from the relationship of flow resistance, expressed by hydraulic losses described by the Chézy velocity coefficient, the value of which, in the model and in nature, should be the same. Expressing the value of the Chézy velocity coefficient with the Manning roughness coefficient and introducing the Strickler parameter, it was shown that the coarse sand used in the laboratory bed models the flow resistance corresponding to the resistance generated by gravel in nature. The verification of the calculated size of scouring was based on popular formulas from Russian literature by Begam and Volčenkov [16], Laursen and Toch's [20] from the English, and use in Poland according to the Regulation ... (Journal of Laws of 2000, No. 63, item 735) [32].

Keywords: bridge, pier, scour, forecast, model, calculations.

[1] Assoc. Prof., Eng., Warsaw University of Life Sciences WULS-SGGW, Institute of Civil Engineering, ul. Nowoursynowska 159, 02-787 Warsaw, Poland, e-mail: slawomir_bajkowski@sggw.edu.pl, ORCID: https://orcid.org/0000-0002-7010-0600

[2] DSc., PhD., Eng., Warsaw University of Life Sciences WULS-SGGW, Institute of Civil Engineering, ul. Nowoursynowska 159, 02-787 Warsaw, Poland, e-mail: marta_kiraga@sggw.edu.pl, ORCID: https://orcid.org/0000-0001-9729-4209

[3] DSc., PhD., Eng., Warsaw University of Life Sciences WULS-SGGW, Institute of Civil Engineering, ul. Nowoursynowska 159, 02-787 Warsaw, Poland, e-mail: janusz_urbanski@sggw.edu.pl, ORCID: https://orcid.org/0000-0001-7689-3667

1. Introduction

The dimensions of the space under the load-bearing structure of water road bridge crossings depend on the transport route parameters and on the hydraulic conditions of the water flow in the crossed stream [1, 7, 11, 14]. The distance of the front walls of the abutments determines the clearance length of the bridge. According to the Regulation in force in Polish law ... [32], the bridge clearance considering design discharges is determined under the bed stability conditions, taking into account the forecasted bed erosion, or excluding bed scouring of the river. The flow of water through bridge cross section may take place in the absence of damming, as well as with damming up water above the crossing. Flow resistance under the bridge also depends on the ice cover [21] and debris that can accumulate on the piers [7, 9, 15, 31] and on bridge spans [33], wind vawes [26] and flow regime [37]. The flow resistance under bridges is significantly influenced by piers whose supports are fixed elements (1 in Fig. 1) introduced into the stream.

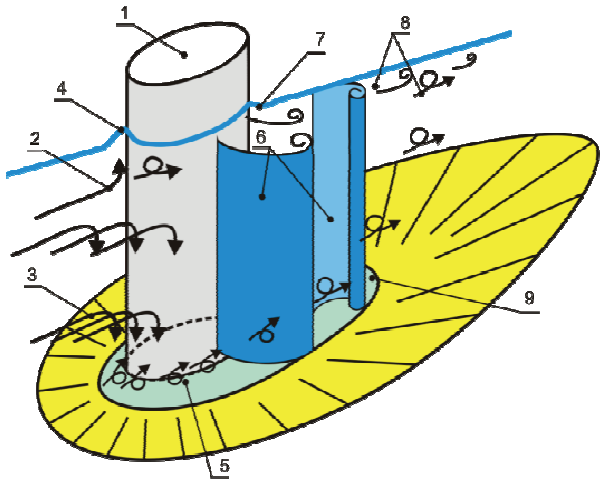

Fig. 1. Form flows around a cylindrical bridge pier: 1 – pier, 2 – up flow, 3 – down flow, 4 – bow wave, 5 – horseshoe vortices, 6 – initial vortices, 7 – farwater vortices, 8 – lee-wake vortices, 9 – local scouring area

Under such conditions, the water stream flowing to the pier head is divided into a part flowing upwards (2 in Fig. 1) and moving towards the riverbed (3 in Fig. 1), while flowing around the pier structure along its edges [34]. Water masses directed upwards create a bow wave in front of the pier (4 in Fig. 1). The stream going towards the bed and hitting it causes the formation of a horseshoe vortex (5 in Fig. 1) [10; 30]. Initial vortices (6 in Fig. 1) form from the inlet section in the line of the

pier face at the depth of the stream, which take the form of a lee-wake vortex. These vortices moving down towards the bed, together with the farwater vortices (7 in Fig. 1) and the horseshoe vortices moving upwards, form a vortex area of the water footprint (8 in Fig. 1). The water footprint vortices intensity decrease rapidly with a distance from the pier, causing sediment settlement below the pier across its width. This phenomenon is especially visible downstream broad piers [6].

2. Materials and methods

2.1. Stream parameters and scour shape

The river bed scouring formation around the bridge piers is an effect of the strong interaction between the turbulent water flow in the pier region. A horseshoe vortex moving around the pier base increases the flow velocity in the bottom area, and the vortices carry the eroded material downstream. When the soil loss is greater than the amount of sediment flowing into the area of the pier [35, 36], the riverbed around the pier starts scouring to form a pothole whose surface creates the reinforced bed zone [13, 31], which is less prone to scouring phenomenon and stabilizes the piers in the event of other threats [2]. The scouring of the riverbed with time [24] and its increasing depth reduce the force of horseshoe vortices, which reduces the ability to lift the soil from the pier's surroundings. This process takes place differently under “live-bed” conditions than under “clear-water” conditions [6, 22, 23], when the resulting pothole is replenished with transported material, then there is an equilibrium between eroded and approaching sediment, which stops the scouring of the bed. Under “clear-water” conditions, when the shear stresses on the bed soil caused by the horseshoe vortices become less than the critical shear stress, the pothole stabilizes its dimensions [6, 22, 23].

2.2. Parameters of bed material

No significant changes in aggregate grain size distribution were observed during the tests, which is confirmed in the publication by Kiraga [18]. Coarse quartz sand was used as the bed material, detached and then transported during the flow of water, the graining characteristics of which were determined on the basis of sieve analysis and the applicable soil classification (Table 1). The coarse sand ($d_{50} > 0{,}5$ mm), used on the model was uniformly grained ($U < 6$, $C_k \cong 1$ according to PN-EN ISO 14688-2: 2006 [29] and well sorted ($\varepsilon \leq 4 \div 5$). Taking into account that $C_d < 1.0$ and $d_{50}/d_{10} = 1.75$ and $d_{90}/d_{50} = 1.09$, the sediment was characterized by the predominance of a smaller

fraction than d_{50}. The soil degree of compaction I_D ranged within the limits of 0.77÷0.82, that is the soil was in a compacted state.

Table 1. Diameters, graining curve indexes and features of the bed material used in the model (own study)

No.	Diameters (mm)		Graining curve indicators	Parameters of the bed material
1	2		3	4
1	d_5	0.45	$C_k = 1.4$ $U = 1.77$ $\varepsilon = 2.70$ $C_d = 0.62$	$\rho_r = 2.65$ g·cm^{-3} $\rho_0 = 1.63$ g·cm^{-3} $\rho_d = 1.57$ g·cm^{-3} $e = 69.0\%$ $w = 4.01\%$ $p = 41.0\%$ $I_D = 0.77 \div 0.82$
2	d_{10}	0.52		
3	d_{30}	0.82		
4	d_{50}	0.91		
5	d_{60}	0.92		
6	d_{85}	0.98		
7	d_{90}	0.99		
8	d_{95}	1.20		

Note: C_k – particle size ratio determined according to PN-B-02481: 1998 [29], U – soil heterogeneity index determined according to PN-EN ISO 14688-1: 2006 [27], ε – Knoroz heterogeneity index, C_d – Kollis domination parameter, ρ_r (g·cm^{-3}) – specific density of the soil skeleton, ρ_0 (g·cm^{-3}), ρ_d (g·cm^{-3}) – the bulk density of the soil skeleton, e (%) – porosity index, w (%) – soil moisture, p (%) – porosity, I_D (–) – compaction degree.

2.3. Methodology of laboratory tests

The model similarity theory of physical phenomena was used to transfer the results obtained on the model to an object in nature. Two systems were defined, that is, the first model – according to own laboratory research, marking its values with the index M, and the second one in nature – obtained from the conversion of model quantities into a natural object, marking its values with the index N. When modeling and transforming the results from the model into a real object, the geometric, kinematic and dynamic similarities were taken into account [4, 38]. The linear scale of modeling α_i (M_i – modeling scale factor) of the model and natural object is expressed by the ratio I_M of the linear dimension of the model and I_N of the corresponding dimension in nature:

Geometric relations of the research flume and the model. Laboratory tests were carried out in a flume $B_M = 0.58$ m wide, with a bed filled with thick sand $d_{50} = 0.91$ mm, in which a cylindrical pier with a diameter of $b_M = 0.05$ m was built [19]. The flume with a depth of $T_M = 0.60$ m was filled with sediment with a layer 0.20 m thick, and the remaining depth $H_M = 0.40$ m was used to obtain the water depth. The total length of the bed with a sandy was 6.0 m, and the scoured length of the test section was $L_R = 2.20$ m. The length of the scoured bed above the forehead and along the pier was $L_M = L_g + L_s = 0.55$ m (Fig. 2).

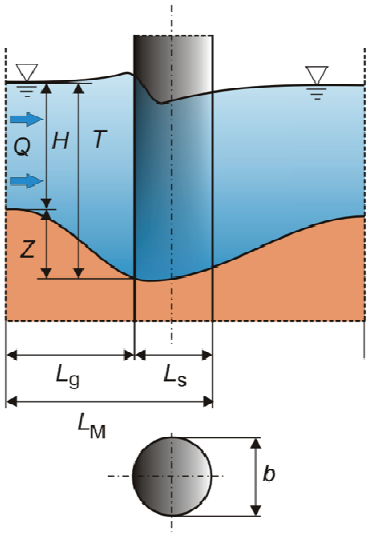

Fig. 2. Pier model and scour parameters: H – water depth, Z – maximal scour depth, Q – water discharge, b – pier diameter, L_g – upstream scour length, L_s – middle scour length, L_M – maximum scour sector

The laboratory water installation was equipped with valves and an electromagnetic flow meter with a flow rate measurement accuracy of ±1%. Spike water gauges with a reading accuracy of $\pm 1 \cdot 10^{-4}$ m (±0.01 cm) were used to measure the water and scour levels. Laboratory measurements of scouring were performed for 19 test series. The minimum, average and maximum values of the measurement variables and dimensionless values obtained from experimental tests are summarized in Table 2. The dimensions of the research riverbed determine the acceptable ranges of the adopted modeling scale coefficients. The scoured test section of the laboratory bed had relative dimensions, related to the pier width, equal to: length of $L_M/b_M = 11.0$, width $B_M/b_M = 11.60$ and depth $T_M/b_M = 11.0$ (the lower index M means dimensions on the model). The obtained maximum relative dimensions of the bed of the scouring, given in Table 2, show that the length of the bed on which the maximum scouring took place and its height are greater than the largest lengths of the analyzed bed of the scouring and the water depth in the place of scouring, obtained in the tests.

The relative bottom width of the scour was equal to the relative bed test width in each case. This proves that the studied phenomenon was a flat flow, and the use of the results is limited to crossings where the scouring extends to the planes of the face walls of the bridge abutments. This form of scouring occurs in small bridges, defined with a width not exceeding 10 m. With the model bed width $B_M = 0.58$ m, the modeling scale of a small field bridge limited by the width of the laboratory bed is $\alpha_L \cong 0.059$ (10.00/0.58; 1:17).

Table 2. Parameters of the physical model and ranges measuring values (own study)

No.	Model parameters	Values		
		Minimal	Average	Maximal
1	2	3	4	5
1	Q (m^3s^{-1})	0.020	0.031	0.043
2	H (m)	0.080	0.107	0.150
3	Z (m)	0.065	0.092	0.131
4	L (m)	0.105	0.223	0.505
5	T (m)	0.165	0.199	0.241
6	H/b	1.600	2.140	3.000
7	Z/b	1.306	1.839	2.626
8	T/b	3.294	3.979	4.826
9	L/b	2.100	4.463	10.100
10	B/b	11.600	11.600	11.600
11	Fr (–)	0.420	0.610	0.752
12	Re (–)	2.35E+04	3.52E+04	4.84E+04
13	I_z (‰)	0.70	2.65	4.80

Note: Q (m^3s^{-1}) – water discharge, H (m) – *w*ater depth, Z (m) – maximal scour depth, L (m) – total scour length, T (m) – *w*ater depth at the point of maximum scour depth, Fr (–) – Froude number, Re (–) – Reynolds number, I_z (‰) – water surface slope

The scale selection is also limited by the minimum measurement depth on the model, which should not be less than 5 cm, that is $H_{Mmin}/b_M = 1.0$. The minimum stream depth $H = 0.08$ m obtained in the tests on the model gave the relative minimum depth of the stream in the upper station $H/b_M = 1.6$, and in the place of maximum scouring it was $T/b_M = 3.294$, which means that the requirement to obtain minimum water depths was met. The ranges of the measured quantities, and especially the ratios of their maximum values, are the basis for establishing a simple or non-uniform modeling scale. Modeling scale factors M_X:M_Y:M_Z determine the relations of the dimensions of the research position, L_M:B_M:T_M respectively. The research bed had dimension relations equal to (L_M:B_M:T_M) (1.00:1.05:1.00). In the tests, the ratios of the maximum values (L_{max}:B_{max}:T_{max}) were equal (2.2:2.5:1.0) respectively. The dimensions differentiation is not so large to analyse the phenomenon on a non-uniform scale. The task qualifies for testing the "short" type model [38]. As Majewski [38] states, the distortion of the scale is usually performed for "long" models, in relation to the H dimension of the water depth and it is recommended that this coefficient should not be greater than 5. In case of the described own research, such situation did not occur, because Reynolds number was higher than the pollutant limit, therefore the task was analyzed for the uniform scale, assuming the scale factor $M_X = M_Y = M_Z = M$.

Geometric modeling scale. In the presented research, the bed deformation process is shaped by the interaction of two areas: disturbances in the velocity field of the stream formed around the flowed

pier and susceptibility of the sediment to erosive processes. The first area of the velocity field is shaped by the system of local declines of the water table, especially in the area of the bow wave, lee-wake vortices and the horseshoe vortex developing at the base of the pier. The second area is characterized by density, particle size distribution 30] and sediment grain system. The interconnection of these areas indicates that the basic tested variables are the water surface system/profile and the related bed shape. This system reflects the total flow resistance [4], expressed by the n ($m^{-1/3}s$) coefficient of the bed surface roughness according to Manning, determined by the following formula [3]:

(2.1) $$n = \frac{1}{k_{St}} = \frac{1}{\frac{21.1}{\sqrt[6]{d_{50}}}} = \frac{\sqrt[6]{d_{50}}}{21.1}$$

where:

k_{St} ($m^{1/3}s^{-1}$) – Strickler's flow resistance coefficient,

$d_{50\%}$ (m) – representative diameter of the bed material grains.

The representative diameter of the sediment d_{50M} for the model and d_{50N} for the natural object are entered, respectively. The necessary linear scale of the model $\alpha_L = \alpha_i$,, or the dimensions of a natural object, is selected using the roughness factor criterion, according to the formula:

(2.2) $$\alpha_n = \frac{n_M}{n_N} = \frac{\frac{\sqrt[6]{d_{50M}}}{21.1}}{\frac{\sqrt[6]{d_{50N}}}{21.1}} = \sqrt[6]{\frac{d_{50M}}{d_{50N}}} = \alpha_L^{1/6}$$

(2.3) $$\alpha_L = \frac{L_M}{L_N} = \alpha_n^6$$

The roughness coefficient n_M determined for d_{50M} = 0.91 mm of the sediment used in the research model in the laboratory physical tests is n_M = 0.0148 $m^{-1/3}s$. Majewski [38] indicates in his work that the use of sand in laboratory tests is allowed for modeling in the nature of the sediment of large dimensions. Table 3 summarizes the calculations of the modeling scales for various types of bed material in order to transform the results into a natural object.

Table 3. Modeling scale factor (own study)

No.	Soil type	Identification of the soil fraction	Diameter range	d_{50N} (mm)	n_N ($m^{-1/3}s$)	M_L (–)	α_L (–)
1	2	3	4	5	6	7	8
1	Fine sand	FSa	0.2÷0.63	0.42	0.0129	0.5	2.193
2	Labolatory sand	CSa	$d_5 = 0.45$ $d_{95} = 1.20$	0.91	0.0148	1.00	1.000
3	Coarse sand	CSa	0.63÷2.0	1.32	0.0157	1.4	0.692
4	Gravel	Gr	2.0÷63	32.5	0.0268	**35.7**	0.028
5	Fine gravel	FGr	2.0÷6.3	4.15	0.0190	4.6	0.219
6	Medium gravel	MGr	6.3÷20	13.2	0.0230	**14.5**	0.069
7	Coarse gravel	CGr	20÷63	41.5	0.0279	45.6	0.022
8	Rocks	Co	63÷200	132	0.0338	144.5	0.007

The obtained modeling scale coefficients values (column 7 of Table 3) indicate that the sediment used during laboratory tests enables the results to be transformed into field objects with beds created in gravel formations. The modeling scale factor related to the average gravel grains size should be assumed as equal to M_L = 35.7. Due to the fact that the laboratory material was well sorted, the modeling scale factor was also calculated for the individual gravel fraction groups. The modeling scale factor related to the average grain size of fine gravel is M_L = 4.6, for coarse gravel it should be assumed as equal to M_L = 45.6. The article presents analyzes of the maximum scour depths for an object in nature for the fraction of medium gravel for which the scale factor of 14.5 was obtained. M_L = 15 was assumed for the calculations, which gives the scale α_L = 0.067. It is a scale factor similar to the 1:17 value determined from the dimensions of the research bed. Scour modeling in nature, in sandy soils with the condition $\rho_{rM} = \rho_{rN}$ ($M_{\rho r}$ = l) requires finer bed material use in the laboratory. The 1:144 scale obtained for the rock fraction indicates the possibility of a large impact of the scale effect on the obtained results, as well as the difficulty of mapping the flow conditions in the rocky beds in the laboratory.

Assuming a constant unit mass force on the model and in nature; $g_M = g_N$ (M_g = 1.0) and using the same liquid in the model and in nature; $\rho_{wM} = \rho_{wN}$ ($M_{\rho w}$ = 1.0), the dependencies determining the velocity and flow rate scales, as a function of the length scale:

$$\alpha_V = \alpha_L^{1/2} \tag{2.4}$$

$$\alpha_Q = \alpha_L^{5/2} \tag{2.5}$$

For scouring on real objects modeling approach, three forms of water movement in the test bed were considered, mapping different conditions in the field (Fig. 3).

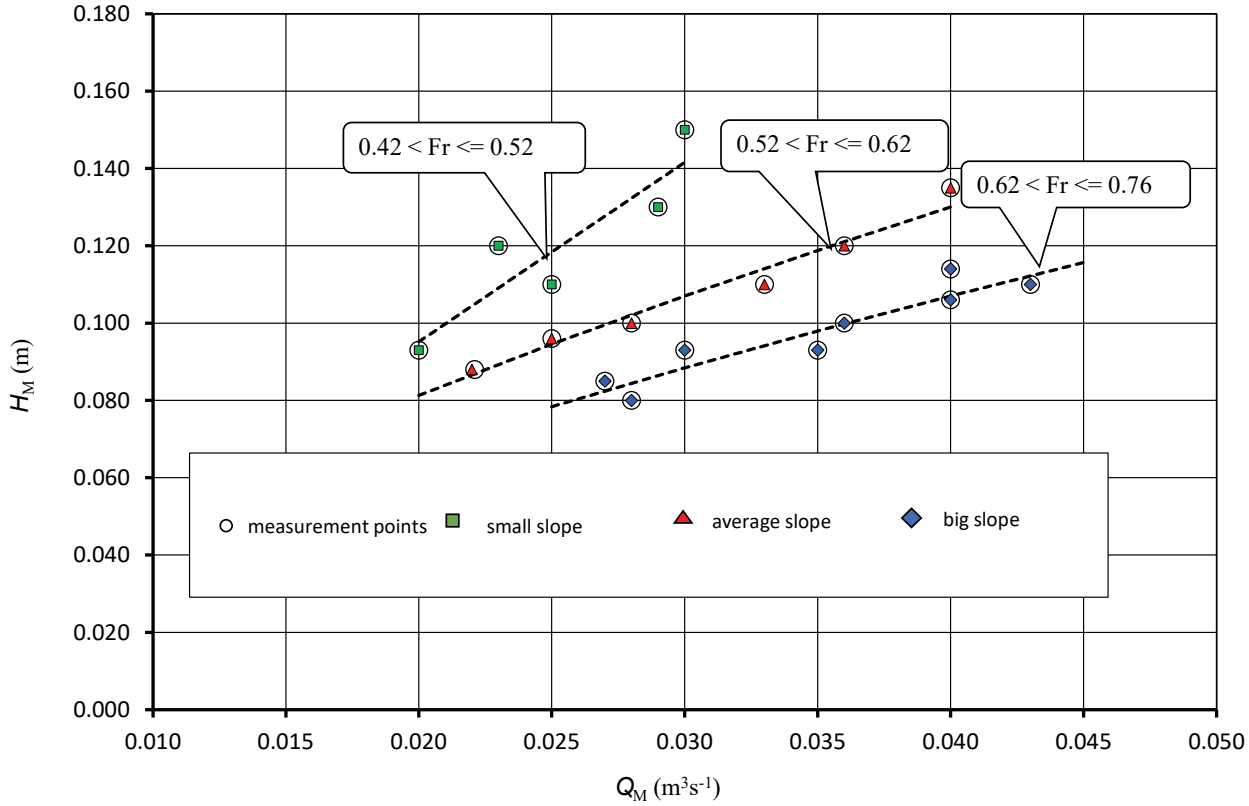

Fig. 3. Discharge curves of the laboratory model flume: F1 – for low riverbed slope, F2 – for medium riverbed slope, F3 – for high riverbed slope

These forms were defined according to the obtained value of the Froude number. The values of the Froude number on the model correspond to the values of the same parameter in nature [25]. In the area of measurement points, three forms of flow were distinguished, reflecting three branches of the bed capacity curve, differing in the values of the Froude number and the riverbed slope (Fig. 3):

- F1 – for $0.42 < Fr \leq 0.52$ for a riverbed slope of $0.70‰ < I_z \leq 1.50‰$,
- F2 – for $0.52 < Fr \leq 0.62$ for a riverbed slope of $1.50‰ < I_z \leq 3.10‰$,
- F3 – for $0.62 < Fr \leq 0.76$ for a riverbed slope of $3.10‰ < I_z \leq 4.80‰$.

Laboratory model and field object. Laboratory tests were performed at a fixed pothole after 8 hours of the experiment. With the longer duration of the experiment, the increase in the pothole depth and the volume of the eroded material was insignificant [18]. Table 4 summarizes the measured values of hydraulic parameters and the depth of scouring on a physical laboratory model and a forecast for the field object.

Table 4. Hydraulic quantities and scour depths for laboratory measurements and the forecast for the field object on the scale $\alpha_L = 0.067$ (1:M_L = 1:15) (own study)

No.	Laboratory model				Field object				Flow form
	Q (m^3s^{-1})	H (m)	V_M (ms^{-1})	Z (m)	Q (m^3s^{-1})	H (m)	V_N (ms^{-1})	Z (m)	
1	2	3	4	5	6	7	8	9	10
1	0.020	0.093	0.371	0.081	17.43	1.40	1.436	1.21	F1
2	0.022	0.088	0.433	0.077	19.26	1.32	1.677	1.15	F2
3	0.023	0.120	0.330	0.065	20.04	1.80	1.280	0.98	F1
4	0.025	0.096	0.449	0.078	21.79	1.44	1.739	1.16	F2
5	0.025	0.110	0.392	0.083	21.79	1.65	1.518	1.25	F1
6	0.027	0.085	0.548	0.090	23.53	1.28	2.121	1.35	F3
7	0.028	0.080	0.603	0.095	24.40	1.20	2.337	1.43	F3
8	0.028	0.100	0.483	0.073	24.40	1.50	1.870	1.09	F2
9	0.029	0.130	0.385	0.082	25.27	1.95	1.490	1.22	F1
10	0.030	0.093	0.556	0.091	26.14	1.40	2.154	1.36	F3
11	0.030	0.150	0.345	0.085	26.14	2.25	1.336	1.27	F1
12	0.033	0.110	0.517	0.084	28.76	1.65	2.003	1.26	F2
13	0.035	0.093	0.649	0.124	30.50	1.40	2.513	1.86	F3
14	0.036	0.100	0.621	0.127	31.37	1.50	2.404	1.90	F3
15	0.036	0.120	0.517	0.086	31.37	1.80	2.003	1.28	F2
16	0.040	0.114	0.605	0.121	34.86	1.71	2.343	1.82	F3
17	0.040	0.106	0.651	0.096	34.86	1.59	2.520	1.43	F3
18	0.040	0.135	0.511	0.080	34.86	2.03	1.979	1.20	F2
19	0.043	0.110	0.674	0.131	37.47	1.65	2.610	1.97	F3

2.4. Methodology of calculations of the scour depth with empirical formulas

The general formula for calculating the maximum scouring depth, various modifications of which are used in engineering calculations, includes functions describing the nature of the velocity field, the bridge crossing geometry and the stream depth, as well as the coefficients: the influence of the shape of the pier and its position in relation to the current, characterizing the ground of the crossing and the type of and the arrangement of group piers, the coefficient characterizing the relationship between the crossing dimensions and the sediment, and the dimension characterizing the width of a single pier or group of piers [5, 6, 12]. In the analyzes, the results of own model studies and empirical formulas obtained from laboratory and field tests described by Begam and Volčenkov [16], given in the Regulation... [32] and presented by Laursen and Toch [20]. The fixed parameters of the crossing are: $b_N = 0.75$ m, $B_N = 8.7$ m, $d_N = 0.01365$ m (13.65 mm). $n_N = 0.0232$ $m^{-1/3}s$.

The formula Begam and Volčenkov [16], also given by Dąbkowski, Skibiński and Żbikowski [17], takes into account the differentiation of the scouring process in the conditions of sediment transport as well as in its absence. It includes the formulas for two cases of scouring formation: without transport and with transport of sediment. This allows for the adaptation of the proposed formulas to

laboratory conditions, performed both in stands with sediment dosing devices, and in their absence. The presented formulas refer to the beds formed in a wide range of soils: fine-grained (sands), medium-grained (gravel) and coarse-grained (rock). For a single cylindrical pier with a diameter b, Begam and Volčenkov's [16] formula takes the form:

$$Z_{\mathrm{Be}} = M \cdot C_{\mathrm{Be}} \cdot \varphi \cdot K_{\mathrm{Be}} \cdot b \tag{2.6}$$

where:

M – coefficient indicating the status of the calculations performed, for the initial forecast: $M = 1.0$ for scouring around cylindrical piers $M = 1.15$ for long piers with shapes other than cylindrical,

C_{Be} – coefficient depending on the type of soil and the velocity ratio V_o/V_n, V_o (ms^{-1}) – vertical velocity in an undeveloped section in front of the pier face, V_n (ms^{-1}) – non-scouring velocity, for non-cohesive soils,

φ – coefficient considering the ratio of the water depth H under the conditions of the non-scoured bed to the diameter b of a single cylindrical pier,

K_{Be} – coefficient taking into account the parameters S, f and the shape of the pier expressed as the ratio of the length L_f of the pier structure or group of piers to the width b and the position of the pier axis in relation to the inflow direction expressed by the angle α_u, S – is considering the relative water depth for diagonal piers, f – is considering the position of the pier's longitudinal axis in relation to the direction of water inflow, expressed by the angle α_u of the support slope, for a cylindrical pier $f = 0$ regardless of the bevel angle of the piers,

b (m) – support structure width, for a single cylindrical pier is assumed equal to its diameter $b = d = 0.75$ m, and for long piers it is the width of the support structure, calculated perpendicularly to the flow direction.

Taking into account the constant values, the final form of formula (2.6) for the conditions occurring on the studied natural object of the bridge crossing, takes the following form:

$$Z_{\mathrm{Be}} = 1.00 \cdot C_{\mathrm{Be}} \cdot \varphi \cdot K_{\mathrm{Be}} \cdot 0.75 \tag{2.7}$$

The formula according to the Regulation ... [8, 32] contains the formula for calculating the Z_{Ro} of the maximum local scouring depth under the bridge, which depends on the shape of the pier, velocity in the bed before the bridge, type of soil and direction of water inflow to the pier:

(2.8) $$Z_{\mathrm{Ro}} = K_1 K_2 (a + K_3) \frac{V_o^2}{g} - C_{\mathrm{Ro}}$$

where:

K_1 – the coefficient depending on the pier shape type, for the most common shapes is given in table, for the considered single cylindrical pier $K_1 = 10.00$,

K_2 – coefficient as a function of the expression V^2/gb_z where: b_z is the equivalent width of a group of piers, for the considered case of a single cylindrical pier $b_z = b$.

a – coefficient taking into account the velocity distribution in the cross-section of the river, for bridge supports located in the main river bed $a = 0.6$,

K_3 – coefficient depending on the ratio of the water depth in the scoured riverbed to the pier equivalent width h_r/b_z, where: h_r – stream depth in the scoured riverbed, b_z – pier's equivalent width. The deepening of the river bed in the bridge section expresses the permissible degree of scouring of the bridge section P. For the foundation placed directly on the ground, the permissible degree of scouring is $P = 1.0$, hence $h_r = H$. For cylindrical pillars at any bevel angle, the value $b_\mathrm{z} = b$,

C_{Ro} (m) – the value of which depends on the type of soil underlying the riverbed, for loose soils $C_{\mathrm{Ro}} = 30\ d_{90}$, for the soil of the substrate of the object in nature $d_{90\mathrm{N}} = 0.0148$ m, $C_{\mathrm{Ro}} = 0.446$ m.

For bridge structures located in valleys with a low slope, the Z_{Ro} value calculated according to formula (2.8) is reduced by 20%. Considering this, for the natural bed, the final local scouring value was set at 0.80 of the value calculated according to the formula (2.8). The final form of the formula (2.8) for the conditions occurring in the tested natural object of the bridge crossing is:

(2.9) $$Z_{\mathrm{Ro}} = 0.8 \left(10.0 \cdot K_2 (0.6 + K_3) \frac{V_o^2}{g} - 0.446\right)$$

The formula Laursen and Toch [20] has been used to estimate the predicted maximum scouring around all intermediate bridge piers since the early 1970s, and despite its simplicity it has gained great popularity and acceptance from engineering communities in the United States. It is used in the case of single and group piers located in rivers with an even-grained bed material.

(2.10) $$\frac{z_{La}}{b} = K_s K_\alpha m \left(\frac{H}{b}\right)^n$$

where:

K_s – pier face shape coefficient, for a circular face $K_\mathrm{s} = 0.9$,

K_α – coefficient depending on the position of the pier's longitudinal axis with respect to the stream, for a cylindrical pier, the bevel angle $\alpha_u = 0$, hence $K_\alpha = 1.0$,

m, n – coefficients of the equation describing the dependence of the depth of scouring as a function of the stream depth, for the base rectangular pier $m = 1.5$ and $n = 0.3$.

By introducing the determined values of the coefficients into Eq. (2.10), the scouring around a single cylindrical pier is obtained in the form:

$$Z_{\mathrm{La}} = \left[0.9 \cdot 1.50 \left(\frac{H}{b}\right)^{0.300}\right] b \tag{2.11}$$

3. Results and discussion

The projected depths of scouring of the bed at the pier on the model in the scale 1:15 and on the object in nature are summarized in Table 4. For the flows and the corresponding water depths in the riverbed, the values of the projected scour obtained from the physical model range from 0.98 m to 1.97 m. In the scope of the distinguished flow forms, the scour occurred in the following value ranges: for F1 from 0.98 m to 1.27 m, for F2 from 1.09 m to 1.28 m and for F3 from 1.35 m to 1.97 m. It follows that the mapping of the flow conditions occurring in natural gravel beds with the sandy material of the coarse sand fraction in the laboratory should be limited to the form of supercritical motion, with the Froude number not greater than 0.62. Laursen and Toch [20] indicate that for the material used on the bed in the diameter range from 0.44 mm to 2.25 mm, such tests can be carried out for higher Froude number values, but not exceeding Fr = 0.8. Chavan et al. [30] conducted research for Fr = 0.25÷028, and Howard et al. [12] for Fr = 0.20÷0.60.

Scour calculations in the natural riverbed for the gravel fraction according to the Eq. (2.7) by Begam and Volčenkov [16], and the Eq. (2.9) prepared according to the Regulation... [32] and Eq. (2.11) by Laursen and Toch [20] are summarized in Table 5 and Fig. 4. The presented formula of [20] Eq. (2.7) makes it possible to calculate scouring in soils with a wide range of grain size, from fine sands to rock fractions. For a bed in gravel soils, without division into fraction groups, the value of the predicted scouring depth varies to a small extent, from 0.94 m to 1.04 m (column 6 in Table 5). It should be noted that the established modeling scale factor was adopted for the medium gravel fraction. Relatively small values of scouring dimensions may result from incomplete representation of the actual conditions of the formation of scouring in gravel formations because coarse sand was used in the model.

Table 5. Scour depth of the riverbed around the cylindrical pier for the scale factor M_L = 15 (own study)

No.	Flow form	V_n (ms^{-1})	Eq. (2.7) Begam and Volčenkov [16]			Eq. (2.9) Regulation… [32]			Eq. (2.11) Laursen and Toch [20]	
			C_{Be} (–)	φ (–)	Z_{Be} (m)	K_2 (–)	K_3 (–)	Z_{Ro} (m)	H/b (–)	Z_{La} (m)
1	2	3	4	5	6	7	8	9	10	11
1	F1	1.337	1.01	1.09	0.94	0.63	0.35	0.64	1.86	1.22
2	F2	1.319	1.03	1.08	0.96	0.60	0.38	0.98	1.76	1.20
3	F1	1.425	0.99	1.12	0.96	0.65	0.23	0.36	2.40	1.32
4	F2	1.348	1.03	1.09	0.97	0.59	0.33	1.00	1.92	1.23
5	F1	1.395	1.01	1.11	0.97	0.62	0.27	0.65	2.20	1.28
6	F3	1.308	1.06	1.07	0.98	0.55	0.39	1.64	1.70	1.19
7	F3	1.288	1.08	1.06	0.99	0.53	0.43	2.06	1.60	1.17
8	F2	1.362	1.04	1.10	0.98	0.57	0.31	1.13	2.00	1.25
9	F1	1.454	1.00	1.14	0.98	0.62	0.19	0.53	2.60	1.35
10	F3	1.337	1.06	1.09	0.99	0.55	0.35	1.60	1.86	1.22
11	F1	1.507	0.99	1.16	0.99	0.64	0.14	0.34	3.00	1.41
12	F2	1.395	1.04	1.11	1.00	0.56	0.27	1.23	2.20	1.28
13	F3	1.337	1.09	1.09	1.02	0.51	0.35	2.16	1.86	1.22
14	F3	1.362	1.08	1.10	1.02	0.52	0.31	1.89	2.00	1.25
15	F2	1.425	1.04	1.12	1.01	0.56	0.23	1.16	2.40	1.32
16	F3	1.407	1.07	1.12	1.03	0.53	0.25	1.66	2.28	1.30
17	F3	1.382	1.08	1.11	1.03	0.51	0.28	2.00	2.12	1.27
18	F2	1.468	1.03	1.14	1.02	0.56	0.18	1.04	2.70	1.36
19	F3	1.395	1.09	1.11	1.04	0.51	0.27	2.08	2.20	1.28

The values obtained from the formula included in the Regulation... [32] constitute a divergence. The calculations used the formula recommended for a large bridge in lowland rivers. Within the scope of the tested water depths, the maximum scouring depth calculated according to Eq. (2.9) varies to a large extent, i.e. from 0.34 m to 2.16 m (column 9 in Table 5). For the motion form F1 (Fr = 0.42÷0.52), the smallest depths of the maximum scouring were obtained, ranging from 0.34 m to 0.65 m. When the stream in the riverbed was characterized by the motion form F2 with the number Fr = 0.52÷0.62, the maximum scouring depth was obtained in the range from 0.94 m to 1.23 m. For the motion form F3 (Fr = 0.62÷0.76), the maximum scouring depths were the largest and ranged from 1.64 m to 2.16 m. It follows that the method of forecasting local scouring included in the Regulation... [32] should be used only for the recommended conditions, i.e. in lowland rivers whose beds are made of alluvial sandy deposits.

The research described by Laursen and Toch [20] is a broad and comprehensive analysis of cases of the scour formation under the influence of various factors, included in Eq. (2.11) and other ones considered, and which did not show sufficient grounds to include them in the formula. These include: soil graining of the bed material, a wide range of structural solutions for the piers, the impact of floating pollutants accumulating in front of the front wall of the piers, the form of water movement, including water velocity, the applied bed reinforcements around the piers. However,

Laursen and Toch [20] did not introduce these factors in the resulting formula, probably treating them as irrelevant at this level of formula refinement. The values obtained from the Eq. (2.11) calculations are characterized by a curvilinear dependence of the relative scour depth on the relative depth of water in the river. Within the scope of the tested water depths, the maximum scouring depth calculated according to Eq. (2.11) varies from 1.17 m to 1.41 m (column 11 in Table 5)
The relative values of the maximum depths of scouring (Z/b) depending on the relative depth of the stream (H/b) are shown in Fig. 4. The points showing the measurement results obtained in the own research for the flow forms F1 and F2 are grouped together. The points for the F3 flow form are grouped separately. The boundary of separation is the hydraulic conditions defined by the Froude number equal to 0.62. The results of the measurements showed that the physical modeling of the scouring process with the use of natural material gives reliable results for supercritical movement with the Froude number not exceeding 0.62. Above this value, the mapping of the flow phenomena occurring in the field of coarse-grained soils using the model with a sandy bed is subject to high measurement uncertainty. For the forms F1 and F2 of the flow in the riverbed, in the range of Froude's number Fr < 0.62, the equation is:

(3.1) $$\frac{z_{\mathrm{N}}}{b} = 1.438\left(\frac{H}{b}\right)^{0.117} \qquad r = 0.280,\ R^2 = 0.061$$

For the formula of Begam and Volčenkov [16], the calculation points for the conditions on the site are in the lowest scouring zone. In his procedure, the author does not distinguish between the fraction groups of the gravel material and does not separate the fine, medium and coarse gravel fractions. For this reason, it is reasonable that relatively smallest scouring was obtained for the fraction of gravels, considering the following equation:

(3.2) $$\frac{z_{\mathrm{Be}}}{b} = 1.290\left(\frac{H}{b}\right)^{0.036} \qquad r = 0.188,\ R^2 = 0.044$$

The model tests performed best reflected the conditions for the formation of scouring indicated in the methodology contained in the Regulation ... [32] for beds with F2 movement with the number Fr = 0.52÷0.62. The equation applied to calculate the scouring in the beds formed in the gravel formations shows a decrease in the impact of increasing stream depths on the depth of the maximum scouring:

(3.3) $$\frac{z_{\mathrm{Ro}}}{b} = 1.210\left(\frac{H}{b}\right)^{0.236} \qquad r = 0.335,\ R^2 = 0.161$$

It follows that in order to verify the method recommended in the Regulation... [32] ,the model should be provided with a broad front of scouring conditions, i.e. not limited by the walls of bridge abutments, as is the case of large bridge crossings with stream piers in wide beds. In other cases, the research task should be considered as "flat".

Introducing the determined values of the coefficients into the Eq. (2.11) by Laursen and Toch [20], we obtain equations for the calculation of the scouring around a single cylindrical pier in the form:

(3.4) $$\frac{z_{La}}{b} = 1.350\left(\frac{H}{b}\right)^{0.300} \qquad r = 0.998;\ R^2 = 1.000$$

4. Conclusions

The collective summary of the model and calculated values of the relative scouring depth (Z/b) as a function of the ratio (H/b) presented in Fig. 4 showed that all values for the modeled conditions and ranges of application of the formulas converge to each other.

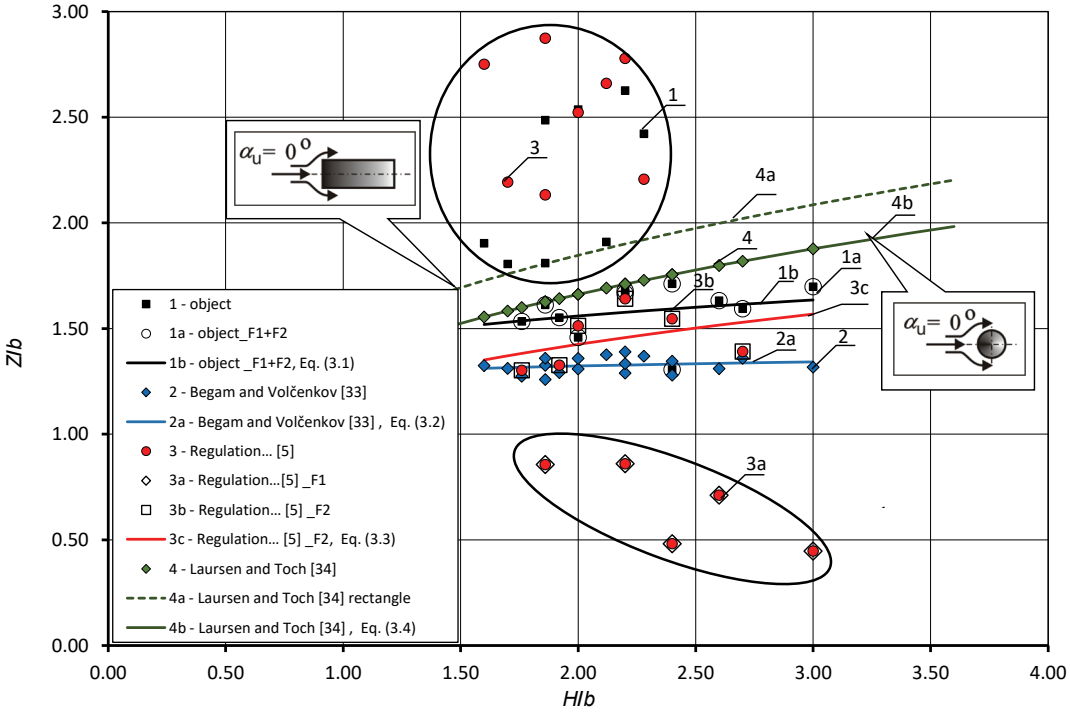

Fig. 4. The depths of scour according to laboratory tests and empirical formulas: 1 – object, 1a – object flow forms F1 i F2, 1b – Eq. (3.1), 2 – Begam and Volčenkov [16], 2a – Eq. (3.2), 3 – Regulation... [32], 3a – Regulation... [32] flow form F1, 3b – Regulation... [32] flow form F2, 3c – Eq. (3.3), 4 – Laursen and Toch [20], 4a – Laursen and Toch [20] rectangle, 4b – Eq. (3.4)

The forecast using the formula contained in the Regulation... 32] for a large bridge has the largest range of obtained values and they are from 0.34 m to 2.16 m. The results of the model tests were similar for the forms F1 and F2 motion, and the form of F3 motion is difficult to model in the laboratory with the use of coarse sand. The analyzes should exclude results developed outside the scope of application of calculation formulas and some results of laboratory tests, in which the reliability of the modeling of flow conditions in nature cannot be stated. The analyzes were limited to the tested range of relative filling volumes of the H/b bed from 1.60 to 3.00 in the bed and the corresponding Froude number varies from 0.42 to 0.75. For the examined object, the smallest values of scouring were obtained from the Eq. (2.7), and the largest ones according to the Eq. (2.11). The model values for the forms of movement F1 and F2 in the riverbed and according to the Eq. (2.9) recommended in the Regulation... [32] are characterized by a lower precision in determining the parameters of relative scouring on a field object. Their values as well as the developed regression curves Eq. [3.1] and Eq. [3.3] were in the area between the values according to Eq. [3.2] by Begam and Volčenkov [35] and Eq. [3.4] by Laursen and Toch [20].

The conducted research and the analysis of their results demonstrated that:

1. The use of model studies in the conditions of the river bed mapping with the use of natural sandy material on the model is reasonable in the assessment of scouring on field objects whose beds are made of coarse-grained soils.
2. Physical modeling of the scouring phenomenon should be performed in the conditions of mapping the similarity of phenomena in nature and on the model, for the case presented in the article it was for the Froude number not greater than 0.62.
3. The developed equations are recommended to be used in practice in the scope of the water depth in the range from 1.60 to 3.0 of diameters of the cylindrical pier.
4. Physical modeling of the form and dimensions of the pothole in the vicinity of the piers of large bridges should be carried out in laboratory beds with a width greater than the extent of the pothole being formed.
5. Relatively small scouring values obtained according to the formula of Begam and Volčenkov [16] may result from incomplete modeling of flow conditions in nature in gravel formations – coarse sand was used in the test bed.
6. The method according to the Regulation ... [32] should be used only for the conditions in which it is recommended, that is occurring in lowland rivers whose beds are made of alluvial sandy deposits.

Acknowledgement:

The article was developed as a result of a research project no. 2020/04/X/ST8/01504 financed by the National Science Centre, Poland.

References

[1] A. A. ven Te Chow, "Open-Bed Hydraulics," New York: McGraw-Hill Book Company, 1959.
[2] A. Duchaczek, D. Skorupka, "Evaluation of Probability of Bridge Damage as a Result of Terrorist Attack," *Archives of Civil Engineering*, vol. 2, pp. 215–227, Jun. 2013. https://doi.org/10.2478/Ace-2013-0011
[3] A. Radecki-Pawlik, P. A. Carling, E. Słowik-Opoka, R. Breakspeare, "On sand-gravel bed forms investigation within the mountainous river," *Infrastruktura i Ekologia Terenów Wiejskich*, vol. 3, pp. 119–134, 2005.
[4] A. Szuster, B. Utrysko, "Hydraulika i podstawy hydromechaniki," Warszawa: Wydawnictwo Politechniki Warszawskiej, 1986.
[5] B. Hodi, "Effect of Blockage and Densimetric Froude Number on Circular Bridge Pier Local Scour," in *Electronic Theses and Dissertations,* vol 79, Windsor, Ontario, Canada, 2009.
[6] B. Liang, S. Du, X. Pan, L. Zhang, "Local Scour for Vertical Piles in Steady Currents: Review of Mechanisms, Influencing Factors and Empirical Equations," *Journal Marine Science Engineering*, vol. 8, pp. 4–27, Dec. 2020. https://doi.org/10.3390/jmse8010004
[7] B. Melville, "The Physics of Local Scour at Bridge Pier," in Fourth International Conference on Scour and Erosion, Civil and Environmental Engineering, The University of Auckland, Auckland, vol. K-2, pp. 28–40, 2008.
[8] B. Utrysko, S. Bajkowski, L. Sz. Dąbkowski, „Światła mostów i przepustów. Zasady obliczeń z komentarzem i przykładami," Wrocław – Żmigród: Instytut Badawczy Dróg i Mostów, Poland, 2000.
[9] D. Panici, G. A. M. De Almeida, "Formation, growth, and failure of debris jams at bridge piers," *Water Resources Research*, vol. 54, pp. 6226–6241, Aug. 2018. https://doi.org/10.1029/2017WR022177
[10] D. Poggi, N. O. Kudryavtseva, „Non-Intrusive Underwater Measurement of Local Scour Around a Bridge Pier," *Water*, vol. 11, pp. 2063–2074, Oct. 2019. https://doi.org/10.3390/w11102063
[11] G. J. C. M. Hoffmans, H. J. Verheij, "Scour Manual," Rotterdam: A. A. Balkema, 1997.
[12] H. D. Copp, J. P. Johnson, "Riverbed Scour at Bridge Pier," Final Report WA-RD 118.1. Washington State Department of Transportation, Technical Report Standard Title Page, Washington State Department of Transportation. Planning. Research and Public Transportation Division in cooperation with the United States Department of Transportation, Pullman: Federal Highway Administration, 1987.
[13] H. D. Copp, J. P. Johnson, J. L. Mcintosh, "Prediction methods for local scour at intermediate bridge piers," *Transportation Research Record*, vol. 1201, pp. 46–53, 1988.
[14] H. N. C. Breusers, A. J. Raudkivi, "Scouring. Hydraulic Design Considerations. Hydraulic Structures Design Manual," London & New York: Association For Hydraulic Research Association 2. Taylor & Francis Group, 1991.
[15] J. Schalko, C. Lageder, V. Schmocker, V. Weitbrecht, R. M. Boes, "Laboratory Flume Experiments on the Formation of Spanwise Large Wood Accumulations: Part II–Effect on local scour," *Water Resources Research*, vol. 55, pp. 4871–4885, May 2019. https://doi.org/10.1029/2019WR024789
[16] L. G. Begam, G. Volčenkov, "Vodopropusknaâ sposobnost' mostov i trub," Moskva: Transport, 1973.
[17] L. Sz. Dąbkowski, J. Skibiński, A. Żbikowski, „Hydrauliczne podstawy projektów wodnomelioracyjnych," Warsaw: Państwowe Wydawnictwo Rolnicze i Leśne, 1982.
[18] M. Kiraga, "Local scour modelling on the basis of flume experiments," *Acta Scientiarum Polonorum Architectura*, vol. 18, no. 4, pp. 15–26, Mar. 2019. https://doi.org:10.22630/ASPA.2019.18.4.41
[19] M. Kiraga, J. Urbański, S. Bajkowski, "Adaptation of Selected Formulas for Local Scour Maximum Depth at Bridge Piers Region in Laboratory Conditions," *Water*, vol. 12, pp. 2663–2682, Sept. 2020. https://doi.org/10.3390/w12102663
[20] M. Laursen,. A. Toch, "Scour around piers and abutments," Bulletin 4, Iowa: Iowa Highway Research Board, USA, 1956.
[21] M. R. Namaee, J. Sui, "Impact of armour layer on the depth of scour hole around side-by-side bridge piers under ice-covered flow condition," *Journal of Hydrology and Hydromechanics*, vol. 67, no. 3, pp. 240–251, Jul. 2019. https://doi.org/10.2478/johh-2019-0010-240
[22] M. S. Fael, G. Simarro-Grande, J. P. Martı´n-Vide, A. H. Cardoso, "Local scour at vertical-wall abutments under clear-water flow conditions," *Water Resources Research*, vol. 42, pp. 10408–10428, Oct. 2006. https://doi.org/10.1029/2005WR004443
[23] M. van Der Wal, G. Van Driel, H. J. Verheij, "Scour manual. Desk study". Delft Hydraulics: Rijkswaterstaat, 1991.

[24] N. A. Obied, S. I. Khassaf, "Experimental Study for Protection of Piers Against Local Scour Using Slots," *International Journal of Engineering*, vol. 32, no. 2, pp. 217–222, Mar. 2019. https://doi.org/10.5829/ije.2019.32.02b.05
[25] N. S. Cheng, M. Wei, "Scaling of Scour Depth at Bridge Pier Based on Characteristic Dimension of Large-Scale Vortex," *Water*, vol. 11, pp. 2458–2466, Nov. 2019. https://doi.org/10.3390/w11122458
[26] O. Link, "Physical scale modeling of scour around bridge piers," *Journal of Hydraulic Research*, vol. 57, no. 2, pp. 227–237, Jul. 2019. https://doi.org/10.1080/00221686.2018.1475428
[27] PN-B-02481: 1998 Geotechnika. Terminologia podstawowa, symbole literowe i jednostki miar. Polski Komitet Normalizacji, Miar i Jakości, Poland, 1998.
[28] PN-EN ISO 14688-1: 2006 Badania geotechniczne. Oznaczanie i klasyfikowanie gruntów. Część 1: Oznaczanie i opis. Polski Komitet Normalizacyjny, Poland, 2006.
[29] PN-EN ISO 14688-2: 2006 Badania geotechniczne. Oznaczanie i klasyfikowanie gruntów Część 2: Zasady klasyfikowania. Polski Komitet Normalizacyjny, Poland, 2006.
[30] R. Chavan, P. Gualtieri, B. Kumar, "Turbulent flow structures and scour hole characteristics around circular bridge piers over non-uniform sand bed beds with downward seepage," *Water*, vol. 11, no. 8, pp. 1580–1597, Jul. 2019. https://doi.org/10.3390/w11081580
[31] R. W. P. May, J. C. Ackers A. M. Kirby, "Manual on scour at bridges and other hydraulic structures". London: CIRIA C551, UK, 2020.
[32] Rozporządzenie z dnia 30 maja 2000 r. Ministra Transportu i Gospodarki Morskiej z dnia 30 maja 2000 roku w sprawie warunków technicznych, jakim powinny odpowiadać drogowe obiekty inżynierskie i ich usytuowanie (Dz.U. 2000 nr 63 poz. 735). Regulation... (Journal of Laws 2000 No. 63 item 735).
[33] S. Bajkowski, "Effect of the Siekierka bridge on the flood flow on Zwoleńka river," *Wiadomości Melioracyjne i Łąkarskie*, vol. 58, no. 1, pp. 23–29, 2015.
[34] S. Oh Lee, S. Ho Hong, "Turbulence Characteristics before and after Scour Upstream of a Scaled-Down Bridge Pier Model," *Water*, vol. 11, pp. 1900–1914, Sept. 2019. https://doi.org/:10.3390/w11091900
[35] S. Bajkowski, "Bed load transport through road culverts," *Scientific Review Engineering and Environmental Sciences*, vol. 2, no. 40, pp. 127–135, 2008.
[36] J. Urbański, "Influence of turbulence of flow on sizes local scour on weir model," *Acta Scientiarum Polonorum Architectura*, vol. 7, no. 2, pp. 3–12, 2008.
[37] W.-G. Qi, F.-P. Gao, "Physical modeling of local scour development around a large-diameter monopile in combined waves and current," *Coastal Engineering*, vol. 83, pp. 72–81, Jan. 2014. https://doi.org/10.1016/j.coastaleng.2013.10.007
[38] W. Majewski, "Hydrauliczne badania modelowe inżynierii wodnej," *Seria publikacji naukowo-badawczych IMGW-PIB*, Instytut Meteorologii i Gospodarki Wodnej Państwowy Instytut Badawczy, Poland, 2019.

Inżynierskie prognozowanie rozmyć miejscowych wokół walcowego filara mostowego na podstawie doświadczeń

Słowa kluczowe: filar, most, rozmycie, prognoza, badania modelowe

Streszczenie:

Celem pracy było wskazanie procedury wykorzystania laboratoryjnych fizycznych badań modelowych rozmyć wokół filarów mostowych dla potrzeb określenia potencjalnego rozmycia koryta rzecznego na terenowych przeprawach mostowych. Wykorzystanie wyników badań laboratoryjnych w prognozowaniu rozmyć wokół filarów nowo projektowanych mostów wymaga uwzględnienia wpływu skali modelu. W warunkach analizowanego zadania skalę modelu ustalono z relacji parametrów granulometrycznych rumowiska wykorzystanego w badaniach modelowych i rumowiska rzecznego w cieku, dla którego prowadzono prognozę rozmyć. Określenie współczynnika nieskażonej skali modelowania według kryterium miarodajnej średnicy rumowiska ogranicza zastosowanie wyników badań na modelach fizycznych do wybranych rodzajów rumowiska rzecznego. Prognozowane głębokości rozmycia dna przy filarze w naturze zostały określone dla obiektu modelowanego w skali 1:15 ustalonej z relacji oporów przepływu, wyrażonych stratami hydraulicznymi opisanymi współczynnikiem prędkości Chezy, którego wartość na modelu i w naturze powinna być taka sama. Wyrażając wartość współczynnika prędkości Chezy, współczynnikiem szorstkości Manninga i wprowadzając parametr Stricklera, wykazano, że piasek gruby zastosowany w korycie laboratoryjnym

modeluje opory przepływu odpowiadające oporom jakie generuje żwir w naturze. Do weryfikacji obliczonych wielkości rozmyć wykorzystano popularne wśród projektantów formuły z literatury rosyjskiej Begama i Volčenkova [35], angielskiej Laursena i Tocha [36] oraz zalecane do stosowania w Polsce według Rozporządzenia… [5]. W rezultacie otrzymano wzory opisujące wielkości rozmyć dla badanego obiektu ze wskazaniem zakresów ich stosowania.

Zbiorcze zestawienie modelowych i obliczonych wartości względnej głębokości rozmycia (Z/b) w funkcji stosunku (H/b) wykazało, że wartości uzyskanych głębokości rozmyć dla modelowanych warunków i zakresów stosowania wzorów są wzajemnie zbieżne. Prognoza z zastosowaniem formuły zawartej w Rozporządzeniu… [5] dla dużego mostu ma największy zakres uzyskanych wartości rozmyć, które zawierają się w przedziale od 0,34 m do 2,16 m. Wyniki badań modelowych były zbliżone do siebie dla form ruchu F1 i F2, a forma ruchu F3 jest trudna do modelowania w warunkach laboratoryjnych z wykorzystaniem piasku grubego. Z analiz wykluczono wyniki opracowane poza zakresem stosowania wzorów obliczeniowych oraz część wyników badań laboratoryjnych, w których nie można stwierdzić wiarygodności odwzorowania na modelu warunków przepływu w naturze. Dla obiektu obliczeniowego najmniejsze wartości rozmyć uzyskano ze wzoru (2.7) Begama and Volčenkova [35], a największe według równania (2.11) Laursena i Tocha [36]. Wartości modelowe dla form ruchu F1 i F2 w korycie obliczone ze wzoru (2.9) rekomendowanego w Rozporządzeniu… [5] charakteryzują się mniejszą precyzją ustalania wartości względnych rozmyć na obiekcie terenowym. Ich wartości, jak też opracowane krzywe regresji (równania 3.1 i 3.3) zawierały się w obszarze pomiędzy wartościami według wzoru (3.2) Begama i Volčenkova [35] oraz według wzoru (3.4) Laursena i Tocha [36].

Received: 2021-01-04, Revised: 2021-02-25